Current Applied Physics 17 (2017) 785–792

Contents lists available at ScienceDirect

Current Applied Physics

journal homepage: www.elsevier.com/locate/cap

# Controlled enzymatic stability and release characteristics of supramolecular chiral peptide amphiphile nanofiber gels

Aygul Zengin, Goksu Cinar, Mustafa O. Guler*

*Institute of Materials Science and Nanotechnology, National Nanotechnology Research Center (UNAM), Bilkent University, Ankara, 06800, Turkey*

ARTICLE INFO

*Article history:*
Received 26 September 2016
Received in revised form
16 February 2017
Accepted 28 February 2017
Available online 2 March 2017

*Keywords:*
Self-assembly
Peptide amphiphile
Supramolecular chirality
Enzymatic stability
Nanofibers
Controlled release

ABSTRACT

Supramolecular bioarchitectures formed by assembly of achiral or chiral building blocks play important roles in various biochemical processes. Stereochemistry of amino acids is important for structural organization of peptide and protein assemblies and structure-microenvironment interactions. In this study, oppositely charged peptide amphiphile (PA) molecules with L-, D- and mixture of L- and D-amino acid conformations are coassembled into supramolecular nanofibers and formed self-supporting gels at pH 7.4 in water. The enzymatic stability of the PA nanofiber gels was studied in the presence of proteinase K enzyme, which digest a broad spectrum of proteins and peptides. The structural changes on the chiral PA nanofibers were also analyzed at different time periods in the presence of enzymatic activity. Controlled release of a model cargo molecule through the chiral PA nanofiber gels was monitored. The diffusivity parameters were measured for all gel systems. Release characteristics and the enzymatic stability of the peptide nanofiber gels were modulated depending on organization of the chiral PA molecules within the supramolecular assemblies.



## 1. Introduction

Chirality is an intrinsic property of molecules due to non-superimposable organization of the atoms on their mirror images either with right- or left-handed positioning [1]. Proteins and peptides found in natural organisms typically consist of L-amino acids, which direct many different biological processes including enzymatic reactions [2], receptor-cell membrane binding [3] and antimicrobial activity [4]. Changing amino acid chirality effects the interaction of peptides with proteolytic enzymes such that the integration of the unnatural D-amino acid into the peptide backbone results in improved biostability to the enzymatic activity at molecular level [5].

The chiral information in amino acids, which are the building blocks of self-assembling peptide molecules can be used as a control on the design of supramolecular peptide assemblies [6,7], which have received wide interest for various biomedical applications due to their inherent bioactivity, biocompatibility and biodegradability [8,9]. The structural organization of the peptide molecules can be modulated by incorporation of the D-amino acids into the peptide backbone [10]. Previously, it was shown that the position of the D-amino acid on the peptide molecule resulted in disturbance of the hydrogen bonding and weak self-assembly properties [11]. On the other hand, the supramolecular peptide gels, which were built via the self-assembly of only D-amino acids showed increased biostability against proteolytic degradation although weak gelation behavior was reported due to the disrupted intermolecular interactions [12]. In another study, stability, biodistribution and toxicity of self-assembled peptide nanofibers with different chirality (L-fibers or D-fibers) were studied [13]. The results of *in vitro* and *in vivo* studies exhibited that supramolecular D-fibers are more stable than L-fibers under physiological conditions. While L-fibers were completely degraded in plasma within 6 h, D-fibers preserved their overall structural integrity in plasma for 24 h. In addition, biodistribution studies revealed that chirality of the self-assembled nanofibers also affected the accumulation of the supramolecular architectures on the organs [13]. In addition, D-amino acids containing dipeptide hydrogelators were also used *in vivo* for controlled drug release applications [14].

Peptide amphiphiles (PAs) consisting of hydrophobic alkyl tail, aliphatic and hydrophilic amino acid residues self-assemble into highly ordered hierarchical nanostructures and supramolecular self-supporting gels due to the noncovalent interactions between the building blocks [15,16]. The straightforward functionalization of

* Corresponding author.
*E-mail address:* moguler@unam.bilkent.edu.tr (M.O. Guler).

http://dx.doi.org/10.1016/j.cap.2017.02.026
1567-1739/

the PA molecules with bioactive epitopes and control on their self-assembly via different factors [17] such as pH change, monomer concentration, temperature or salt concentration make them promising candidates for controlled delivery of the therapeutics [18,19] and tissue engineering applications [20,21].

In this study, we show three different PA nanofiber gel systems to study enzymatic stability and controlled release characteristics depending on their chiral amino acid content. For this purpose, we designed and synthesized oppositely charged self-assembling peptide amphiphile molecules with D and L conformations. Oppositely charged D-, L- and the mixture of D- and L- PA molecules coassembled into high-aspect-ratio nanofibers and supramolecular PA nanofiber gels at pH 7.4 in water without need of any external factor. The enzymatic stability of the supramolecular PA architectures with different chirality were both examined at both nano and bulk scale by TEM imaging and weight loss method, respectively. Furthermore, controlled release of Rhodamine B (RhoB), a model cargo molecule, through the D-, L- and the mixture of D- and L- PA nanofiber gels was monitored with or without proteolytic activity. This study presents a systematic investigation of the effect of supramolecular chirality on the release behavior of D-, L- and the mixture of D- and L- PA nanofiber gels, quantitatively. In the light of the controlled release characteristics and estimated transport parameters of a model cargo molecule through the D-, L and the mixture of D- and L- PA nanofiber gels, these architectures with different chirality can pioneer development of smart drug delivery systems for therapeutic applications.

## 2. Experimental section

### 2.1. Material

9-Fluorenylmethoxycarbonyl (Fmoc)-protected amino acids, lauric acid, Wang resin, Rink amide MBHA resin and 2-(1H-benzotriazol-1-yl)-1,1,3,3-tetramethyluronium hexafluorophosphate (HBTU) were purchased from NovaBiochem. Other chemicals including dichloromethane (DCM), dimethylformamide (DMF), acetonitrile, piperidine, acetic anhydride, *N*,*N*-Diisopropylethylamine (DIAE), trifluoroacetic acid (TFA), uranyl acetate and rhodamine B (RhoB) were purchased from Fisher, Merck, Alfa Aesar or Sigma-Aldrich. Proteinase K from *tritirachium album* was purchased from VWR chemicals.

### 2.2. PA synthesis and characterization

Standard Fmoc solid phase peptide synthesis method was used to synthesize lauryl-Val$^{D}$-Val$^{D}$-Ala$^{D}$-Gly-Glu$^{D}$-Glu$^{D}$-Glu$^{D}$-OH (D-$E_3$PA), lauryl-Val-Val-Ala-Gly-Glu-Glu-Glu-OH (L-$E_3$PA) and lauryl-Val$^{D}$-Val$^{D}$-Ala$^{D}$-Gly-Lys$^{D}$-Lys$^{D}$-Lys$^{D}$-Am (D-$K_3$PA), lauryl-Val-Val-Val-Ala-Gly-Lys-Lys-Lys-Am (L-$K_3$PA). D-$K_3$PA and L-$K_3$PA were constructed on Rink Amide MBHA resin while D-$E_3$PA and L-$E_3$PA were constructed on Fmoc Glu(OtBu)-Wang resin. Amino acid couplings were performed with 2 equivalents of Fmoc-protected amino acid, 1.95 equivalents of HBTU and 3 equivalents of DIAE and then the mixture was shaken for 2 h. In order to remove the Fmoc group, the resins were mixed in 20% (v/v) piperidine/DMF solution for 20 min. After each coupling reaction, the unreacted amine groups were acetylated using 10% (v/v) acetic anhydride solution in DMF for 30 min to prevent side reactions. The PAs were cleaved from the resin by using TFA/TIS/$H_2O$ mixture (95:2.5:2.5 ratio) for 2 h and then collected by DCM. The excess TFA and DCM were removed by rotary evaporation. The remaining sample was triturated with diethyl ether overnight at −20 °C. Then, the PA molecules were removed from diethyl ether by centrifugation. The resulting white precipitate was dissolved in Milli-Q water and then freeze-dried. For the characterizations of the synthesized PA molecules, 1 mg of PA sample was dissolved in 1 mL of $H_2O$ with ultrasonication for 15 min. Liquid chromatography-mass spectrometry (LC-MS) analysis of the PAs was performed with Agilent Technologies 6530 Accurate-Mass QTOF system equipped with a Zorbax Extend-C18 column. 0.1% (v/v) ammonium hydroxide in water (A) and 0.1% (v/v) ammonium hydroxide in acetonitrile (B) were used as mobile phase for the analysis of the negatively charged PAs (D-$E_3$PA and L-$E_3$PA); while 0.1% (v/v) formic acid in water (A) and 1% (v/v) formic acid in acetonitrile (B) were used as a mobile phase for the positively charged PAs (D-$K_3$PA and L-$K_3$PA). The flow rate of mobile phase was 0.65 mL/min. For the first 2 min, mobile phase was 98% (v/v) of A, then B increased to 98% (v/v) between 2 and 25 min; and then turned back to 2% (v/v) for the next 2 min. LC chromatogram was obtained at 220 nm. To purify the synthesized peptide molecules, preparative-high performance liquid chromatography (HPLC) was used.

### 2.3. Preparation of the PA nanofiber gels

The PA powders were dissolved in Milli-Q water and sonicated for 15 min to obtain a homogeneous solution with a concentration of 1% (w/v). Prior to the experiments, negatively charged 1% (w/v) L-$E_3$PA or D-$E_3$PA solutions were mixed with the positively charged 1% (w/v) L-$K_3$PA or D-$K_3$PA solutions, respectively with 3:4 volumetric ratio to trigger coassembly of the PAs into supramolecular nanofiber gels (L-$E_3$/$K_3$ or D-$E_3$/$K_3$) at pH 7.4 in water and incubated for overnight. For preparation of the DL-$E_3$/$K_3$ nanofiber gel, 1% (w/v) $E_3$PA and $K_3$PA solutions consisting 50% D- and 50% L-molecules were prepared, and then mixed with 3:4 volumetric ratio, respectively at pH 7.4 in water. DL-$E_3$/$K_3$ nanofiber gel system was

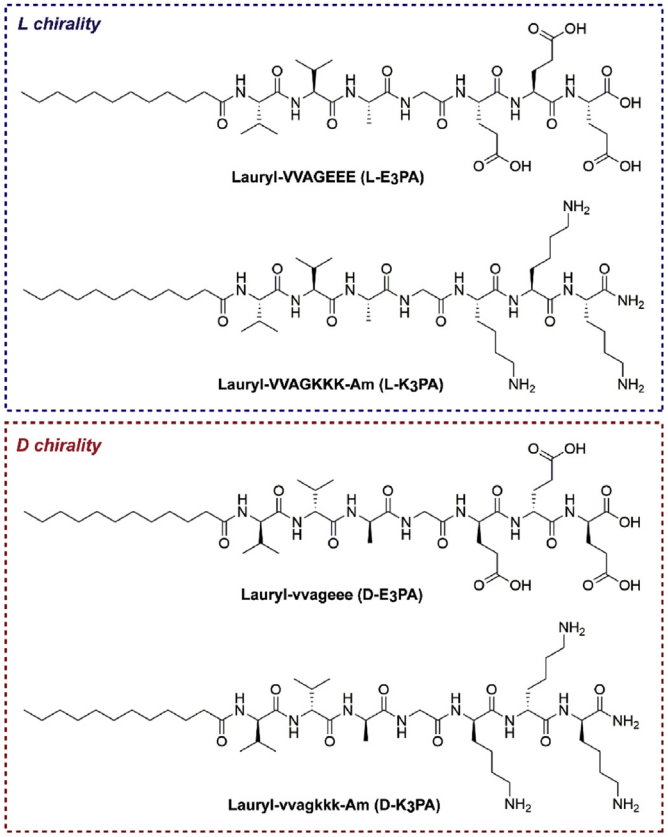


**Fig. 1.** Chemical representations of the oppositely charged PA molecules with L and D configurations.

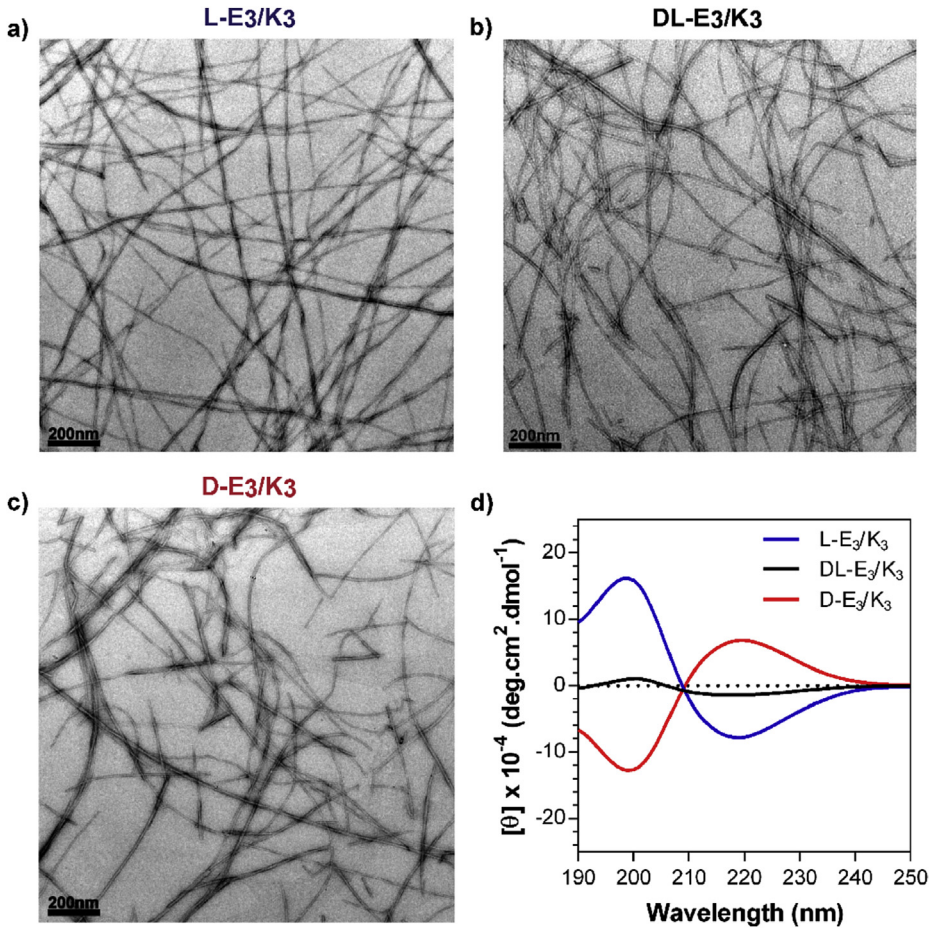


**Fig. 2.** TEM images of the coassembled (a) L-$E_3/K_3$, (b) DL- $E_3/K_3$ and (c) D-$E_3/K_3$ nanofibers. (d) CD spectra of the $E_3/K_3$ coassemblies with L-, D- and the mixture of D- and L-conformations.

also incubated overnight.

### 2.4. TEM imaging

1% (w/v) L-$E_3/K_3$, DL-$E_3/K_3$ and D-$E_3/K_3$ nanofiber gels prepared according to the protocol given above were diluted in 1:30 ratio by addition of Milli-Q water. 10 μL of the diluted gel samples were placed onto TEM grids and waited for 10 min. Excess sample solution was removed from the grid using micropipette. A drop of 2% (w/v) uranyl acetate was casted onto the grid for 5 min and then removed for air-drying of the sample. A FEI Tecnai G2F30 TEM instrument was used to image the coassembled PA nanofibers.

### 2.5. Circular dichroism (CD) analysis

Overnight incubated 1% (w/v) PA nanofiber gels (L-$E_3/K_3$, DL-$E_3/K_3$ and D-$E_3/K_3$) were diluted to 0.033% (w/v) final concentration using distilled water. 300 μL of the diluted samples were filled into 1 mm thick quartz cells; and Jasco J-815 CD spectrophotometer was used for the analysis between 190 and 300 nm with data pitch: 0.1 nm, sensitivity: standard, D.I.T: 1 s, band width: 1 nm, scanning speed: 100 nm/min.

### 2.6. SEM imaging

1% (w/v) L-$E_3/K_3$, DL-$E_3/K_3$ and D-$E_3/K_3$ nanofiber gels prepared on the silicon wafers were dehydrated with the gradually increasing concentrations of ethanol prior to the drying of the PA gels with a Tousimis Autosamdri-815B critical-point-drier (CPD). After the CPD procedure, the nanofibrous architectures were covered with 6 nm electron conductive Au/Pd coating using a sputter. An FEI Quanta 200 FEG scanning electron microscope equipped with an ETD detector was used for the imaging.

### 2.7. Oscillatory rheology

Rheology measurements of 1% (w/v) L-$E_3/K_3$, DL-$E_3/K_3$ and D-$E_3/K_3$ nanofiber gels were performed using an Anton Paar Physica RM301 Rheometer equipped with a 25 mm parallel plate at 25 °C. The sample volume was determined as 250 μL. The distance between the measuring devise and the sample was determined as 0.5 mm. Time sweep analysis of the samples were conducted at constant 10 rad $s^{-1}$ angular frequency and 0.01% strain to examine viscoelastic characteristics of the nanofiber gels. Time sweep analysis of the gels was continued with amplitude sweep test to reveal the linear viscoelastic range (LVR) at constant angular frequency of 10 rad $s^{-1}$ with logarithmically ramping the strain amplitude from 0.01 to 1000%.

### 2.8. Weight based stability measurement of the PA nanofiber gels

300 μL of 1% (w/v) L-$E_3/K_3$, DL-$E_3/K_3$ and D-$E_3/K_3$ nanofiber gels were prepared in glass vials, which were previously weighed. Then, the weights of the vials containing the PA gels were recorded to determine the weight loss of the gels compared to the initial gel amount. After the incubation of the PA gels for 3 h

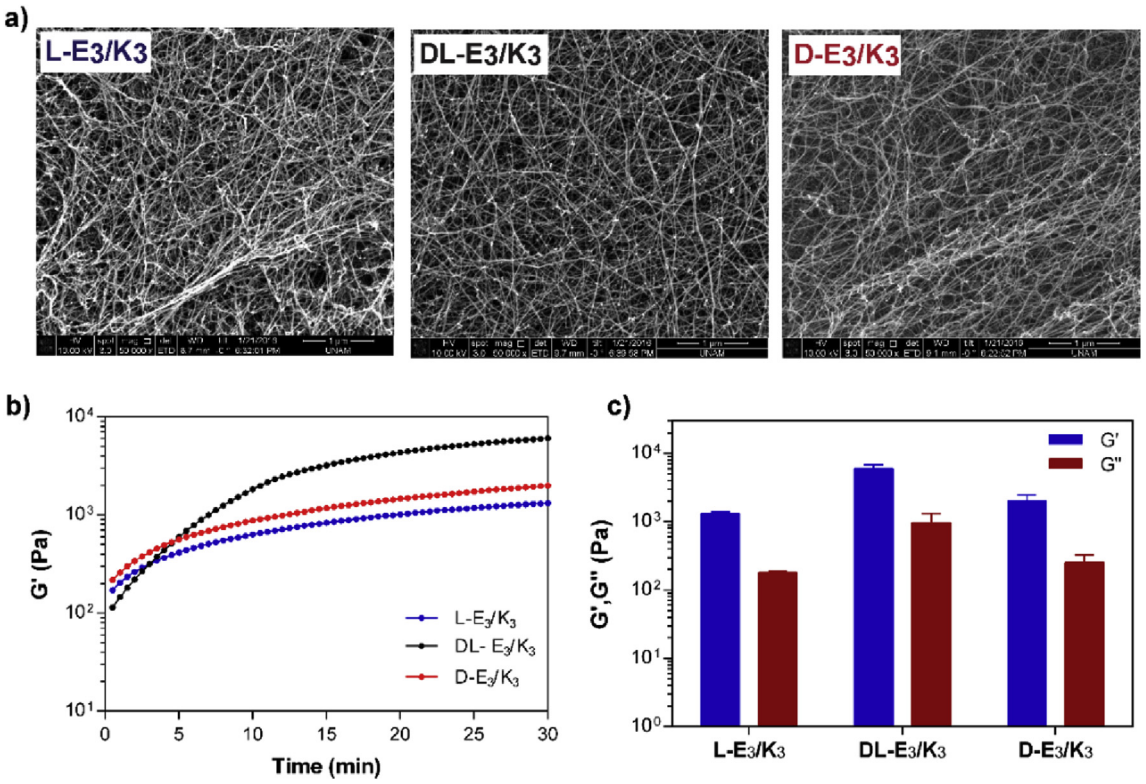


**Fig. 3.** a) SEM images of the L-$E_3/K_3$, DL- $E_3/K_3$ and D-$E_3/K_3$ nanofiber networks. b) Time sweep analysis of the supramolecular PA nanofiber gels; and c) the equilibrium storage (G′) and loss moduli (G″) of the gels.

within the vials; 900 μL of 1 mg/mL proteinase K prepared in 10 mM Tris buffer at pH 7.4 or 10 mM Tris buffer at pH 7.4 without containing the enzyme as control was placed onto the gels carefully. At the defined time intervals, the buffer solutions were removed; and the remaining gels were weighted. Then, the freshly prepared buffer solutions with or without the enzyme containing were replaced onto the gels.

### 2.9. Structural stability of the PA nanofibers

To obtain the PA nanofiber solutions with concentration of 0.1% (w/v), incubated overnight 1% (w/v) L-$E_3/K_3$, DL-$E_3/K_3$ and D-$E_3/K_3$ nanofiber gels were diluted with distilled water. Then, 100 μL of the diluted PA nanofiber solutions were mixed with 900 μL of 1 mg/mL proteinase K in 10 mM Tris buffer or only 10 mM Tris buffer at pH 7.4. Final solutions were incubated for 15 min, 1 day, 7 days and 14 days. At the different time intervals, 10 μL of the samples were taken from the solutions for the structural analysis of the PA nanofibers with TEM imaging.

### 2.10. Controlled release studies

For preparation of Rhodamine B (RhoB) encapsulated 1% (w/v) L-$E_3/K_3$ and D-$E_3/K_3$ nanofiber gels, 1% (w/v) L- or D-$K_3$PA solution (160 μL) was mixed with 20 μL of 0.75 mM RhoB solution; and then 120 μL of 1% (w/v) L- or D-$E_3$PA solution was added into the mixture to trigger coassembly of the PA molecules into supramolecular gels, respectively. For preparation of 1% (w/v) DL- $E_3/K_3$ nanofiber gel; 1% (w/v) D-$K_3$PA (80 μL) and L-$K_3$PA (80 μL) solutions or 1% (w/v) D-$E_3$PA (60 μL) and L- $E_3$PA (60 μL) solutions were mixed separately, and sonicated for 15 min. Initially, 20 μL of 0.75 mM RhoB solution was added into 160 μL of D- and L-mixture of $K_3$PA solution and gelation was triggered upon addition of 120 μL of D- and L-mixture of $E_3$PA solution into the mixture. The samples were prepared in 1 mm quartz cuvettes and incubated for 3 h. Then, 2200 μL of 1 mg/mL proteinase K in 10 mM Tris buffer or only 10 mM Tris buffer was added onto the PA gels for the controlled release of RhoB molecules through the gels at pH 7.4 at room conditions. The concentration of the released RhoB was determined using Varian Cary 100 UV–vis spectrophotometer between 400 and 600 nm. At the defined time intervals, the measured maximum RhoB absorbance was converted into the concentration using a standard calibration curve. All measurements were repeated for three different groups for each gel system.

## 3. Results and discussion

Four different PA molecules consisting of L- or D-amino acids (L-$K_3$PA, L-$E_3$PA, D-$K_3$PA, D-$E_3$PA; Fig. 1) were designed and synthesized according to Fmoc solid phase peptide synthesis method (Figs. S1–S4). All PA molecules consist of three major segments; hydrophobic lauryl tail, aliphatic β-sheet forming domain (-VVA-) and charged amino acid residues (-KKK or -EEE, Table S1). The mixture of positively charged $K_3$PA solution with negatively charged $E_3$PA solution (L-, D- or the mixture of L- and D-chirality, respectively; Table S2) triggered the formation of coassembled PA nanostructures at pH 7.4 in water due to electrostatic, hydrogen bonding and hydrophobic interactions between the PA molecules (Table S2). TEM images of the PA nanostructures (Fig. 2a–c) showed that the coassembly of the oppositely charged PAs resulted in the formation of high-aspect-ratio nanofibers with diameters in the range of 6–10 nm and micrometers in length. In addition, the mixture of the oppositely charged PA molecules with L- and D-conformations did not disturb the nanostructure formation; and revealed supramolecular PA nanoarchitectures (Fig. 2b).

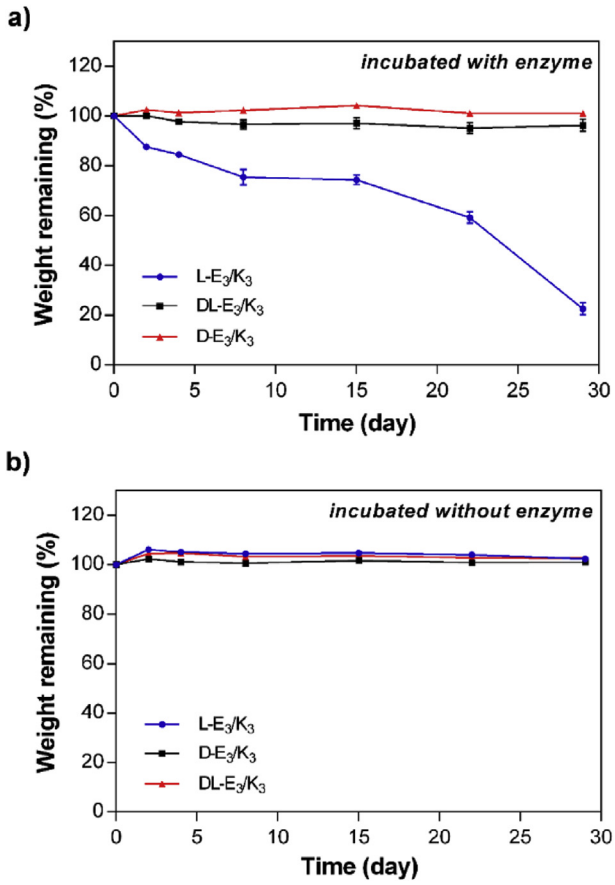


**Fig. 4.** The stability of the L-$E_3/K_3$, DL- $E_3/K_3$ and D-$E_3/K_3$ nanofiber gels incubated (a) with and (b) without proteinase K enzyme solutions.

Circular dichroism (CD) spectroscopy was used to study secondary structure of the supramolecular PA assemblies. The CD spectrum of L-$E_3/K_3$ coassemblies showed twisted β-sheet secondary structure organization [22] of the nanofibers with peaks at around 200 and 220 nm (Fig. 2d). Furthermore, CD spectrum of D-$E_3/K_3$ coassemblies revealed mirror symmetry with respect to the spectrum of L-$E_3/K_3$ coassemblies due to the supramolecular organization of the PA molecules with D-chirality. On the other hand, the positive and negative CD signals of DL-E3/K3 coassemblies at around 200 nm and 220 nm respectively decreased since the system consisted of the PA molecules with the mixture of D- and L-conformations (Fig. 2d). The difference in the number of H-bonds in the L and D- PAs is potentially due to two valine residues. The conformational and dynamic behavior of the valines in L- and D-forms are important for the nature of the H-bonds. The valine side-chains can sterically hinder H-bond formation in the D-form. TEM and CD results revealed that this approach enabled us to obtain coassembled PA nanofibers with similar physical properties and different chirality.

To obtain self-supporting supramolecular PA nanofiber gels, 1% (w/v) oppositely charged D-, L- or the mixture of D- and L- PA solutions were mixed at pH 7.4 in water (Fig. S5). The physical properties of the three-dimensional gel systems were imaged using SEM. The images indicated that D-$E_3/K_3$, L-$E_3/K_3$ and DL- $E_3/K_3$ gel networks have similar three-dimensional nanofibrous architectures, which provide suitable environments for the encapsulation of therapeutics for the controlled delivery applications (Fig. 3a). In addition, viscoelasticity and gel-like characteristics of the resulting PA nanofiber gels were examined using oscillatory rheology. The gelation kinetics of 1% (w/v) L-$E_3/K_3$, DL-$E_3/K_3$ and D-$E_3/K_3$ nanofiber gels were monitored under constant angular frequency and strain. The PA systems reached to an equilibrium within 30 min (Fig. 3b); and revealed gel-like character since storage moduli of the samples (G′) were higher than the loss moduli (G″) (Fig. 3c). When the equilibrium moduli of the gels were compared, slightly higher viscoelasticity was reported for DL-$E_3/K_3$ gel system that could be related with the molecular packing of the PA molecules with D- and L-chirality within the supramolecular mixture (Fig. 3c). To determine the limiting strain amplitude (LSA) values of the gels; amplitude sweep test was performed on the incubated samples at the end of the time sweep. Above LSA, the plastic deformation on the samples were observed and the gel behavior disappeared due to the transition from linear to non-linear viscoelastic regime [23]. LSA of the all groups (Fig. S6) were close to each other, and pointed the similar viscoelasticity under oscillatory stresses.

Stability of the 1% (w/v) L-$E_3/K_3$, DL-$E_3/K_3$ and D-$E_3/K_3$ nanofiber gels under proteolytic degradation was investigated by incubating the supramolecular PA nanofiber gels with proteinase K enzyme, which cleaves peptide bonds with a broad specificity [24]. The PA nanofiber gels were weighed at the determined time intervals by removing the enzyme solution placed onto the gels for 29 days (Fig. 4a). While 1% (w/v) L-$E_3/K_3$ lost approximately 80% of their weight in the presence of the enzyme, DL-$E_3/K_3$ and D-$E_3/K_3$ nanofiber gels preserved their gel integrity through the incubation period (Fig. 4a). Although the half of the DL-$E_3/K_3$ gel system consisting of the PA molecules with 50% D-conformations, the stability under proteolytic degradation was similar to the D-$E_3/K_3$ nanofiber gel system. As a control experiment, 1% (w/v) L-$E_3/K_3$, DL-$E_3/K_3$ and D-$E_3/K_3$ nanofiber gels were also incubated without enzyme containing Tris buffer at pH 7.4. All PA gel systems did not reveal any mass change for 29 days (Fig. 4b) due to selectivity of the proteolytic degradation of the gels based on the supramolecular chirality of the PA architectures.

In addition to weight based stability of the PA nanofiber gels, the change on the nanostructure feature under proteolytic activity were examined via TEM imaging of L-$E_3/K_3$, DL-$E_3/K_3$ and D-$E_3/K_3$ nanofiber solutions incubated with the enzyme solutions at different time periods. Like the bulk weight loss results, DL-$E_3/K_3$ and D-$E_3/K_3$ nanofibers did not show any alteration on the structural properties and presented significant nanofiber stability under proteolytic activity for 14 days (Fig. 5). On the other hand, even after 15 min incubation of L-$E_3/K_3$ nanofibers with the enzyme solution, the structures revealed both fiber and sheet-like nanostructures while DL-$E_3/K_3$ and D-$E_3/K_3$ samples demonstrated nanofibers. Over time, drastic effect of the enzymatic degradation on the structural organization of L-$E_3/K_3$ nanofibers became apparent. The nanofibers and sheets were converted into the smaller spherical aggregates at day 14 (Fig. 5). On the other hand, both DL-$E_3/K_3$ and D-$E_3/K_3$ nanofibers showed enhanced structural stability preserving their nanofibrous organization under enzymatic degradation for 14 days. In addition, all groups were also incubated in Tris buffer solutions at pH 7.4 without enzymatic activity. TEM images of these groups exhibited no significant change on the structural properties of the L-$E_3/K_3$, DL-$E_3/K_3$ and D-$E_3/K_3$ assemblies for 14 days (Fig. S7).

To study controlled release characteristics of the PA nanofiber gels, a small molecule fluorescent probe, RhoB, was used as a model drug molecule and encapsulated within the PA gel system with 100% efficiency during the coassembly of the oppositely charged PA molecules in the supramolecular PA gels. Under proteolytic activity of the proteinase K in Tris buffer at pH 7.4, the highest amount of

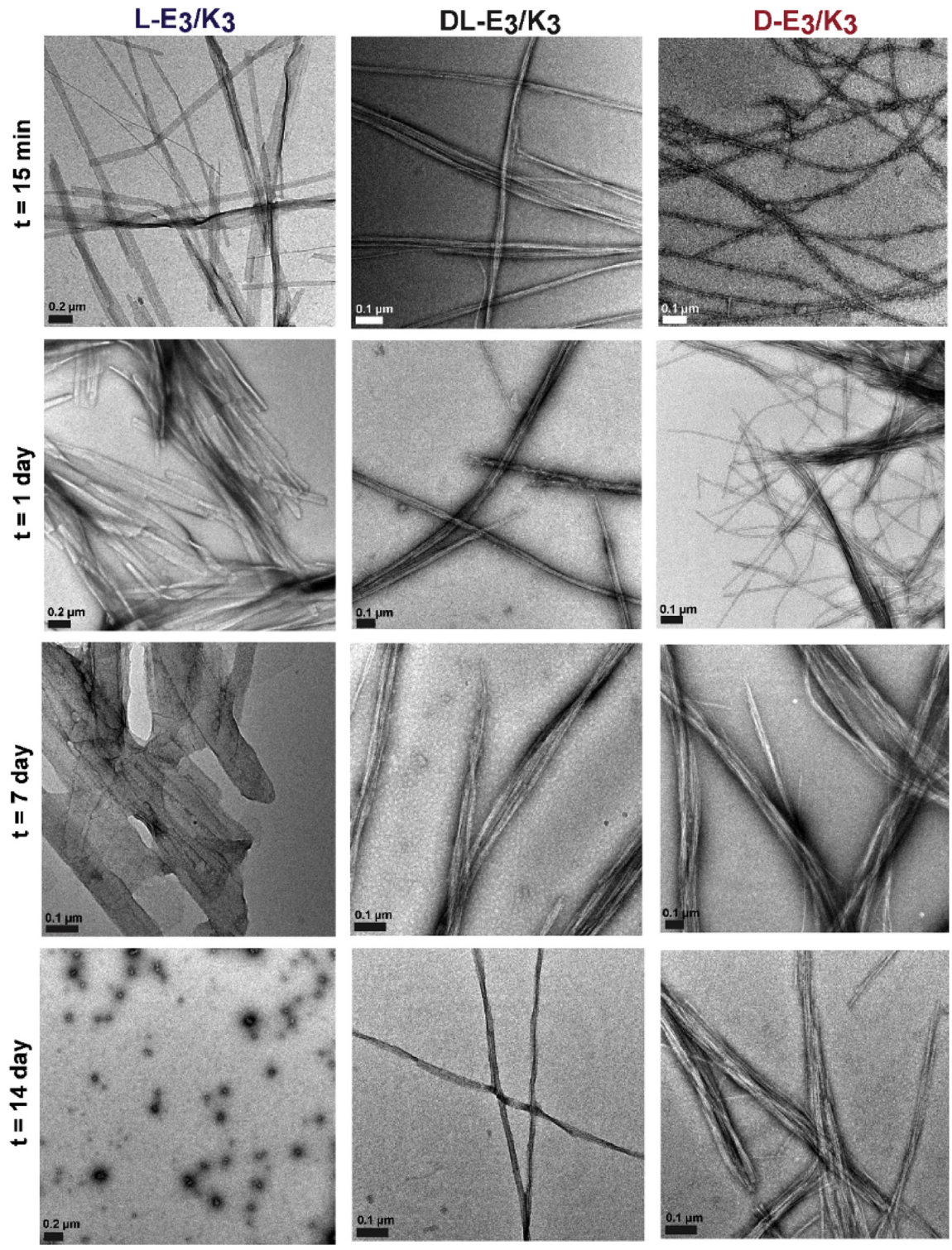


**Fig. 5.** TEM images of the L-$E_3/K_3$, DL- $E_3/K_3$ and D-$E_3/K_3$ nanofibers incubated within proteinase K enzyme solutions for 15 min, 1 day, 7 day and 14 day.

the released molecules was obtained in the L-$E_3/K_3$ nanofiber gels due to their weak proteolytic stability compared to the DL-$E_3/K_3$ and D-$E_3/K_3$ nanofiber gels (Fig. 6a, Fig. S8). On the other hand, although DL-$E_3/K_3$ system revealed similar stability behavior with D-$E_3/K_3$ at both bulk gel and nanoscale, the controlled release of the molecules through DL-$E_3/K_3$ system were higher than the D-$E_3/K_3$ nanofiber gels over time (Fig. 6a). The release of the molecules through the L-$E_3/K_3$, DL-$E_3/K_3$ and D-$E_3/K_3$ nanofibers gels were determined as approximately 75, 41 and 25%, respectively (Fig. 6a). On the other hand, the sustained release of the molecules was monitored through the PA nanofiber gels incubated within the Tris buffer at pH 7.4 without the enzyme as control experiments. Although slightly higher release of the molecules in the L-$E_3/K_3$ nanofiber gels (~34%) were observed compared to DL-$E_3/K_3$ (~23%)

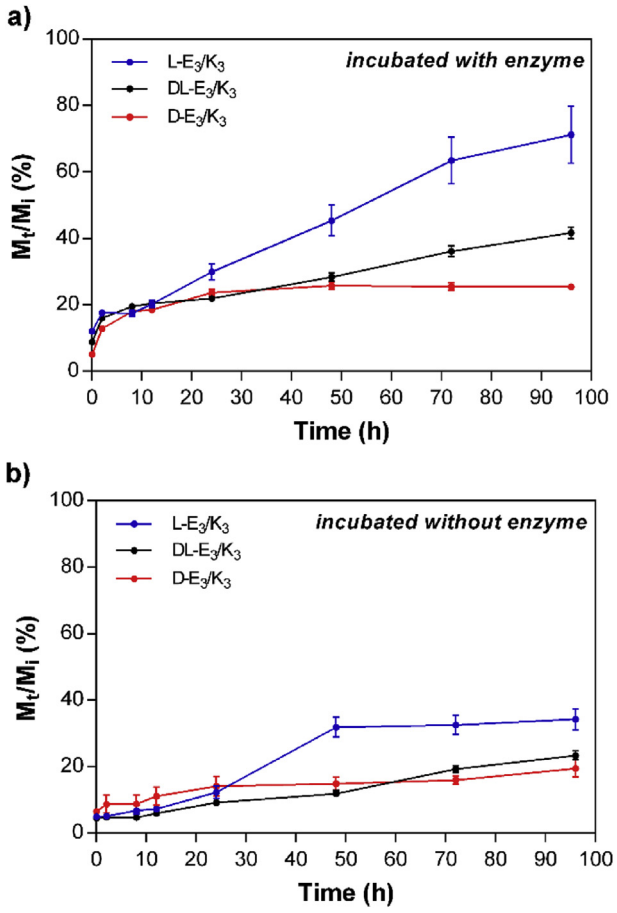


**Fig. 6.** Controlled release of the model Rhodamine B (RhoB) as a model cargo molecule through the supramolecular PA nanofibers gels with different chirality incubated (a) with and (b) without proteinase K enzyme in 10 mM Tris buffer at pH 7.4.

**Table 1**
Diffusion parameters of the model drug molecules released through the supramolecular PA nanofibers gels with different chirality.

| Conditions | $D_{app}$ ($10^{-12}$ $m^2$ $s^{-1}$) | | |
|---|---|---|---|
| | L-$E_3/K_3$ | DL-$E_3/K_3$ | D-$E_3/K_3$ |
| Incubated with enzyme | 2.66 ± 1.13 | 0.89 ± 0.13 | 0.33 ± 0.03 |
| Incubated without enzyme | 0.61 ± 0.20 | 0.28 ± 0.06 | 0.20 ± 0.09 |

and D-$E_3/K_3$ (~19%) (Fig. 6a), the sustained release of the molecules through both L-$E_3/K_3$, DL-$E_3/K_3$ were drastically decreased compared to the systems incubated within the enzyme solutions (Fig. 6a–b).

To estimate apparent diffusivity coefficients the RhoB molecules released through L-$E_3/K_3$, DL-$E_3/K_3$ and D-$E_3/K_3$ for the quantitative comparison of the mass transport properties of the systems; Fick's second law of diffusion for 1D unsteady-state systems given in Eqn. (1) was used [25,26]. In the equation, $D_{app}$, $M_t$, $M_\infty$, H and t was defined as the apparent diffusivity, the cumulative mass of the diffused molecules at time t and infinite and the thickness of the gel, respectively. The estimated apparent diffusion coefficients were given in Table 1.

$$\frac{M_t}{M_\infty} = \left(\frac{16\, D_{app} t}{\pi H^2}\right)^{0.5} \quad (1)$$

Significantly higher diffusivity of the molecules in the L-$E_3/K_3$ nanofiber gels were calculated as 2.66 ± 1.13 × $10^{-12}$ $m^2$ $s^{-1}$ under proteolytic degradation compared to the DL-$E_3/K_3$ and D-$E_3/K_3$ in complementary to the weight based structural stability results. Therefore, the release of the molecules can be modulated depending on the chirality of the peptide molecules and their nanostructures under proteolytic activity because of the chirality on the interactions of the enzyme molecules with the PA coassemblies.

## 4. Conclusions

In this study, we showed three different coassembled PA nanofiber gel systems containing chiral peptide molecules. The coassembled nanofiber formation and gelation behavior of D-, L- and the mixture of D- and L- PA molecules were shown. The results clearly demonstrated that mixing L- and D-form PA molecules significantly enhanced the stability of the coassembled PA nanofibers and supramolecular PA nanofiber gels against the proteolytic activity. While L-$E_3/K_3$ nanofibers were completely degraded during 14 days of incubation with proteinase K, D-$E_3/K_3$ and the DL-$E_3/K_3$ nanofibers exhibited great stability in both enzyme and no enzyme containing buffers. In the case of bulk gel stability, L-$E_3/K_3$ nanofiber gels lost approximately 80% of their weight, while it was negligible for both D-$E_3/K_3$ and DL-$E_3/K_3$ nanofiber gels for 29 days of incubation in the enzyme solutions. Finally, the release experiments of the model molecules through the D-, L and the mixture of D- and L- PA nanofiber gels revealed the tunability of the release characteristics of PA nanofiber gels based on the chirality of the peptide molecules and their nanostructures for controlled delivery of various therapeutics for biomedical applications.

## Acknowledgements

This work was partially supported by TUBITAK (114Z728) and TUBA. A.Z. was supported by TUBITAK-BIDEB 2210-C fellowship and G.C. was supported by TUBITAK-BIDEB 2211-C PhD fellowship. We thank M. Guler and A.S. Dincer for help in TEM imaging.

## Appendix A. Supplementary data

Supplementary data related to this article can be found at http://dx.doi.org/10.1016/j.cap.2017.02.026.

## References

[1] R.S. Cahn, C. Ingold, V. Prelog, Specification of molecular chirality, Angew. Chem. Int. Ed. 5 (1966) 385–415.
[2] M.B. Hoagland, E.B. Keller, P.C. Zamecnik, Enzymatic carboxyl activation of amino acids, J. Biol. Chem. 218 (1956) 345–358.
[3] F.J. Quintana, D. Gerber, I. Bloch, I.R. Cohen, Y. Shai, A structurally altered d,l-amino acid TCRα transmembrane peptide interacts with the TCRα and inhibits t-cell activation in vitro and in an animal model, Biochemistry 46 (2007) 2317–2325.
[4] S. Fernandez-Lopez, H.-S. Kim, E.C. Choi, M. Delgado, J.R. Granja, A. Khasanov, K. Kraehenbuehl, G. Long, D.A. Weinberger, K.M. Wilcoxen, M.R. Ghadiri, Antibacterial agents based on the cyclic D,L-α-peptide architecture, Nature 412 (2001) 452–455.
[5] H. Wang, Z. Feng, B. Xu, D-amino acid-containing supramolecular nanofibers for potential cancer therapeutics, Adv. Drug Deliv. Rev. (2016), http://dx.doi.org/10.1016/j.addr.2016.04.008.
[6] L. Zhang, T. Wang, Z. Shen, M. Liu, Chiral nanoarchitectonics: towards the design, self-assembly, and function of nanoscale chiral twists and helices, Adv. Mater. 28 (2016) 1044–1059.
[7] J. Li, Y. Kuang, Y. Gao, X. Du, J. Shi, B. Xu, D-amino acids boost the selectivity and confer supramolecular hydrogels of a nonsteroidal anti-inflammatory drug (NSAID), J. Am. Chem. Soc. 135 (2013) 542–545.
[8] Z. Luo, S. Wang, S. Zhang, Fabrication of self-assembling D-form peptide nanofiber scaffold d-EAK16 for rapid hemostasis, Biomaterials 32 (2011) 2013–2020.

[9] Z. Luo, Y. Yue, Y. Zhang, X. Yuan, J. Gong, L. Wang, B. He, Z. Liu, Y. Sun, J. Liu, Designer D-form self-assembling peptide nanofiber scaffolds for 3-dimensional cell cultures, Biomaterials 34 (2013) 4902–4913.
[10] I.L. Karle, H.N. Gopi, P. Balaram, Crystal structure of a hydrophobic 19-residue peptide helix containing three centrally located D amino acids, Proc. Natl. Acad. Sci. U. S. A. 100 (2003) 13946–13951.
[11] S. Marchesan, C.D. Easton, K.E. Styan, L.J. Waddington, F. Kushkaki, L. Goodall, K.M. McLean, J.S. Forsythe, P.G. Hartley, Chirality effects at each amino acid position on tripeptide self-assembly into hydrogel biomaterials, Nanoscale 6 (2014) 5172–5180.
[12] X. Li, X. Du, J. Li, Y. Gao, Y. Pan, J. Shi, N. Zhou, B. Xu, Introducing D-amino acid or simple glycoside into small peptides to enable supramolecular hydrogelators to resist proteolysis, Langmuir 28 (2012) 13512–13517.
[13] C. Yang, L. Chu, Y. Zhang, Y. Shi, J. Liu, Q. Liu, S. Fan, Z. Yang, D. Ding, D. Kong, Dynamic biostability, biodistribution, and toxicity of L/D-peptide-based supramolecular nanofibers, ACS Appl. Mater. Interfaces 7 (2015) 2735–2744.
[14] J. Liu, J. Liu, L. Chu, Y. Zhang, H. Xu, D. Kong, Z. Yang, C. Yang, D. Ding, Self-assembling peptide of D-amino acids boosts selectivity and antitumor efficacy of 10-hydroxycamptothecin, ACS Appl. Mater. Interfaces 6 (2014) 5558–5565.
[15] H. Cui, M.J. Webber, S.I. Stupp, Self-assembly of peptide amphiphiles: from molecules to nanostructures to biomaterials, Biopolymers 94 (2010) 1–18.
[16] S. Han, S. Cao, Y. Wang, J. Wang, D. Xia, H. Xu, X. Zhao, J.R. Lu, Self-assembly of short peptide amphiphiles: the cooperative effect of hydrophobic interaction and hydrogen bonding, Chem. Eur. J. 17 (2011) 13095–13102.
[17] X. Zhao, F. Pan, H. Xu, M. Yaseen, H. Shan, C.A. Hauser, S. Zhang, J.R. Lu, Molecular self-assembly and applications of designer peptide amphiphiles, Chem. Soc. Rev. 39 (2010) 3480–3498.
[18] D. Mumcuoglu, M. Sardan, T. Tekinay, M.O. Guler, A.B. Tekinay, Oligonucleotide delivery with cell surface binding and cell penetrating peptide amphiphile nanospheres, Mol. Pharm. 12 (2015) 1584–1591.
[19] R. Mammadov, G. Cinar, N. Gunduz, M. Goktas, H. Kayhan, S. Tohumeken, A.E. Topal, I. Orujalipoor, T. Delibasi, A. Dana, Virus-like nanostructures for tuning immune response, Sci. Rep. 5 (2015).
[20] G. Gulseren, I.C. Yasa, O. Ustahuseyin, E.D. Tekin, A.B. Tekinay, M.O. Guler, Alkaline phosphatase-mimicking peptide nanofibers for osteogenic differentiation, Biomacromolecules 16 (2015) 2198–2208.
[21] M. Sever, B. Mammadov, M.O. Guler, A.B. Tekinay, Tenascin-C mimetic peptide nanofibers direct stem cell differentiation to osteogenic lineage, Biomacromolecules 15 (2014) 4480–4487.
[22] E.T. Pashuck, S.I. Stupp, Direct observation of morphological tranformation from twisted ribbons into helical ribbons, J. Am. Chem. Soc. 132 (2010) 8819–8821.
[23] M. Goktas, G. Cinar, I. Orujalipoor, S. Ide, A.B. Tekinay, M.O. Guler, Self-assembled peptide amphiphile nanofibers and PEG composite hydrogels as tunable ECM mimetic microenvironment, Biomacromolecules 16 (2015) 1247–1258.
[24] W. Ebeling, N. Hennrich, M. Klockow, H. Metz, H.D. Orth, H. Lang, Proteinase K from Tritirachium album limber, FEBS J. 47 (1974) 91–97.
[25] S. Koutsopoulos, L.D. Unsworth, Y. Nagai, S. Zhang, Controlled release of functional proteins through designer self-assembling peptide nanofiber hydrogel scaffold, Proc. Natl. Acad. Sci. U. S. A. 106 (2009) 4623–4628.
[26] Y. Nagai, L.D. Unsworth, S. Koutsopoulos, S. Zhang, Slow release of molecules in self-assembling peptide nanofiber scaffold, J. Control. Release 115 (2006) 18–25.